

## FABRICATION OF GAMMA-IRRADIATED POLYPROPYLENE AND AgNPs NANOCOMPOSITE FILMS AND THEIR ANTIMICROBIAL ACTIVITY

<sup>1</sup>Isabelle Oliveira Berenguer, <sup>1</sup>Washington Luiz Oliani, <sup>1</sup>Duclerc Fernandes Parra, <sup>1</sup>Luiz Gustavo Hiroki Komatsu, <sup>1</sup>Vinicius Juvino dos Santos, <sup>2,3</sup>Nilton Lincopan, <sup>1</sup>Ademar Benevolo Lugao, <sup>4</sup>Vijaya Kumar Rangari

<sup>1</sup>Nuclear and Energy Research Institute, IPEN-CNEN/SP, Av. Prof. Lineu Prestes, 2242, Cidade Universitária, CEP 05508-000, São Paulo – SP, Brazil

\*isa\_berenguer@hotmail.com

<sup>2</sup>Department of Microbiology, Institute of Biomedical Sciences, University of Sao Paulo, CEP 05508-000, São Paulo, Brazil

<sup>3</sup>Department of Clinical Analysis, School of Pharmacy, University of Sao Paulo, Brazil, São Paulo

<sup>4</sup>Center for Advanced Materials Science and Engineering Tuskegee University, AL 36088, USA

**Keywords:** polypropylene, nanocomposites, silver nanoparticles, silicon dioxide, sonochemical

### Abstract

Polymer nanocomposite films of polypropylene and AgNPs were prepared by melt extrusion using twin-screw extruder. These polymer nanocomposites were further modified by  $\gamma$ -irradiation in acetylene at dose of 12.5 kGy. The AgNPs (silver nanoparticles) used in this study were synthesized using sonochemical method from silver nitrate precursor. The polymer nanocomposites were evaluated using differential scanning calorimetry (DSC), X-Ray diffraction (XRD), FTIR spectroscopy and Scanning electron microscopy (SEM). We have also studied the antibacterial activity of these polymer nanocomposite films against two different groups of bacteria- *Staphylococcus aureus* (*S. aureus*; gram-positive bacteria) and *Escherichia coli* (*E. coli*; gram-negative bacteria).

### 1. Introduction

Polypropylene as a commodity represents a versatile material with continuous increasing of applications [1,2]. Radiation modified polypropylene resins (PP) induces degradation, grafting and radiation-induced LCB (long chain branched). It can be taken advantage to the improvement of polymer material quality owing to physical properties. The most significant improvement from radiation induced LCB is on the rheological properties in the polymer processability, especially for the high melt-strength-polypropylene (HMSPP) [3,4]. PP films performing bactericidal effect is an application that is only beginning to be investigated.

Recent survey [5] has been developed in silver nanoparticles deposited on the surface of an extruded film of linear low density polyethylene/cyclo olefin copolymer (LLDPE/COC) blend by ultrasound method. The ultrasound method on the silver deposition on the film surface and the fungicidal effect on the films were evaluated. The author suggested a method for antimicrobial packaging films through AgNPs deposition.

An important aspect of the nanosilver is that the use as is less toxic to human cells compared to other metals, against infections [6]. Therefore, silver nanoparticles possess excellent antimicrobial activity against a broad spectrum of microbes [7]. The silver nanoparticles biocide effect is related to particle size and shape and it is highly dependent on particle dispersion. The presence of macro aggregates can lead to a decrease in antibacterial activity; therefore, good particle dispersion of appropriate dimensions is needed [8].

Sonochemical, among different methods to produce silver nanoparticle composites is one of the most interesting ways. The sonochemical method enables the synthesis of nanoparticles and their deposition on various substrates in a one-step procedure [9]. The irradiation has proven to be an effective aid for the synthesis of nanosized materials [10].

In this project it was used sonochemical method from silver nitrate precursor. To synthesize the silver nanoparticles it was utilized a growth process based on the reduction of silver ion to zerovalent metal atom acting as nucleation sites and Ag nanoparticles on decorated silica sphere core grew using formaldehyde as a reducing agent by N,N-Dimethylformamide (DMF) with the addition of poly(N-vinyl-2-pyrrolidone) (PVP), a protective agent under ultrasound irradiation method. It can be noticed a growth of silver shell on the basis of silver seed dispersed on the surface of silica spheres [11].

One of the effective approaches to improve melt strength and extensibility is to promote chain branches onto polypropylene backbone using gamma radiation and acetylene. Branching and grafting result from the radical combinations during irradiation process [12]. The strain hardening effect of the HMSPP represents an important role in many processing operations like film blowing, blow molding, foam expansion, fiber spinning and thermoforming [13].

The IPEN developed the production of branched PP, based on the grafting of long-chain-branches on PP backbone using acetylene as a crosslink promoter under gamma radiation process. The focus of the present work was the synthesis of silver nanoparticles on silica carrier using sonochemical method for polypropylene nanocomposite films with and evaluation of biocide action versus *Escherichia coli* and *Staphylococcus aureus*.

## 2.1. Materials

The isotactic Polypropylene (iPP) was supplied by Braskem – Brazil in pellets with  $MFI = 2.1 \text{ dg min}^{-1}$ ,  $M_w = 470,000 \text{ g mol}^{-1}$  and density =  $0.905 \text{ g cm}^{-3}$ . The acetylene 99.8% supplied by White Martins S/A, of Brazil, was used to synthesis of modified polypropylene. It was used N,N Dimethylformamide (DMF) analytical grade with molecular weight  $73.09 \text{ g Mol}^{-1}$ . Silica was purchased by Merck. AgNPs were synthesized with silver nitrate in presence of silica, which and the Irganox was provided by Ciba.

The samples evaluated, in Table 1, were PP1 = Polypropylene and PP2 = Polypropylene  $\text{SiO}_2 @ \text{Ag}$  nanocomposite.

**Table 1:** Composition of constituents of polypropylene nanocomposites (wt%)

Samples	Matrix	Dose/kGy	Irganox	AgNPs	Si
PP1	HMSPP	12.5	2	-	-
PP2	HMSPP	12.5	2	0.1	1.0

## 2.2. Methods

### 2.2.1. Radiation process

The irradiation of the PP pellets was performed under acetylene atmosphere in a  $^{60}\text{Co}$  gamma source at dose rate of  $5 \text{ kGy h}^{-1}$ . The polypropylene irradiation was performed at  $12.5 \text{ kGy}$  dose monitored by a Harwell Red Perspex 4034 dosimeter. After irradiation, the samples were heated for 1h at  $90 \text{ }^\circ\text{C}$  to promote the recombination and annihilation of residual radicals [14, 15].

### 2.2.2. Synthesis of $\text{SiO}_2@ \text{Ag-NPs}$ by sonochemical method from silver nitrate precursor

To synthesize the AgNPs with silica, it was used 50 mL of water and 50 mL of the DMF in a 300 mL beaker then added approximately 1000 mg of silica ( $\text{SiO}_2$ ), 200 mg of PVP and 400 mg of silver nitrate ( $\text{AgNO}_3$ ). The beaker with the solution was putted in another larger recipient with cold water for cooling. It was used a Unique ultrasound equipment model DES 500, with a working frequency of 20 kHz and maximum intensity output of 500 Watts. The process was divided in three steps, each one with 30 minutes. Between the steps, it was changed the cooling water to maintain the room temperature. In the final process, the precipitated was washed with distilled water. After washings, it was putted in the stove and dried for 2 hours and stored in a dark container. The synthesis of the silver is presented on Figure 1.



Figure 1. Schematic diagram illustrating the synthesis process of the silver decorated silica ( $\text{SiO}_2 / \text{Ag}$ )

### 2.2.3. Preparations of $\text{SiO}_2 @ \text{Ag-NPs/PP}$ Nanocomposites Films

The HMSPP 12.5 kGy in pellet was mixed with Irganox B 215 ED in a rotary mixer and maintained under this condition for 2 hours. Then the mixture was processed with the addition of silver nanoparticles (AgNPs 0.1% by weight) with silica in a twin-screw extruder Haake co-rotating, model Rheomex PTW 16/25, with the following processing conditions: the temperature profile (feed to die) was  $175\text{-}230 \text{ }^\circ\text{C}$ , with a speed of 100 rpm. After processed, the nanocomposites were granulated in a granulator Primotécnica W-702-3. The PPSiO<sub>2</sub>@Ag-NPs films were produced in blow extruder and the material was placed directly into the hopper of the extruder with a temperature profile (feed to die) of  $175\text{-}220 \text{ }^\circ\text{C}$ , screw speed of 20 rpm and torque of 70-80 Nm. The films were produced with a thickness of  $\sim 0.08 \text{ mm}$ .

## 2.3. Characterization Films

### 2.3.1 Scanning electron microscopy and dispersive spectroscopy

Scanning electron microscopy was done using an EDAX PHILIPS XL 30. In this project, thin coat of carbon was sputtered onto the samples.

### 2.3.2. Fourier transformed infrared spectroscopy

The analyses were performed using attenuation total reflectance accessory (ATR) transmittance in the Thermo Nicolet spectrophotometer, model 380 FT-IR.

### 2.3.3. Differential scanning calorimetry

Thermal properties of specimens were analyzed using a differential scanning calorimeter DSC 822, Mettler Toledo. The thermal behavior of films was obtained by (1) heating from -50 to 280 °C at a heating rate of 10 °C min<sup>-1</sup> under nitrogen atmosphere; (2) holding for 5 min at 280 °C; and (3) then cooling to -50 °C and reheating to 280 °C at 10 °C min<sup>-1</sup>.

### 2.3.4. X-ray diffraction

X-ray diffraction measurements were carried out in the reflection mode on a Rigaku diffractometer Mini Flex II (Tokyo, Japan) operated at 30 kV voltage and current of 15 mA with CuK $\alpha$  radiation ( $\lambda = 1,541841 \text{ \AA}$ ).

### 2.3.5. Determination of antibacterial activity

An aliquot (400  $\mu\text{L}$ ) of a cell suspension of either *Staphylococcus aureus* ATCC 27853 ( $10^6$  cells mL<sup>-1</sup>) or *Escherichia coli* ATCC 25922 ( $10^6$  cells mL<sup>-1</sup>) prepared using the method described in JIS Z 2801 [16] were held in intimate contact with each of the 2 replicates of the test surfaces supplied using a 45 x 45 mm<sup>2</sup> polypropylene film for 24 hours at 37 °C under humid conditions. The size of the surviving population was determined using a method based on JIS Z 2801. The viable cells in the suspension were enumerated by viable cell counts on MacConkey Agar after incubation at 37 °C for 24 hours using a 100  $\mu\text{L}$  sample taken from the test surfaces.

## 3. Results and discussion

### 3.1. Scanning electron microscopy and dispersive spectroscopy

The SEM-EDX results are shown in Figure 2.

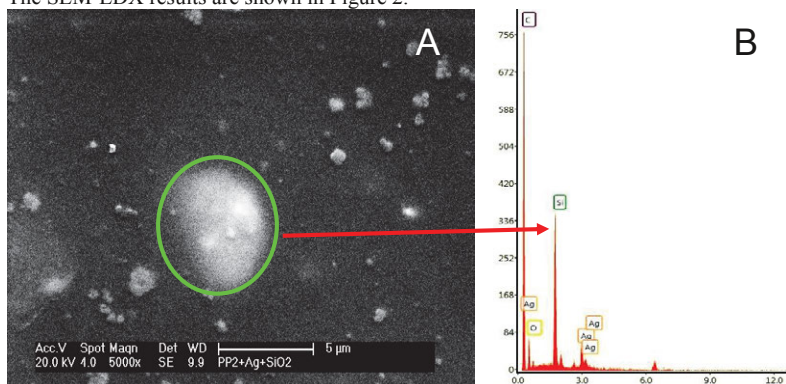


Figure 2. SEM micrograph (A), and EDX of nanocomposite PP2 film (B)

The micrograph of polypropylene nanocomposite film, Figure 2, shows the of SiO<sub>2</sub> particle in which, by sonification, the nanosilver particles grown, as characterized by EDX. Encircled the particle observed is the SiO<sub>2</sub> carrier of nanosilver particles in PP matrix.

### 3.2. Fourier transformed infrared spectroscopy

Figure 3 shows the infrared spectrum of the samples PP1 and PP2.

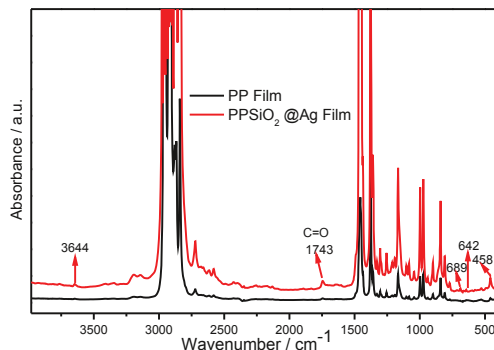


Figure 3. Illustration of the FTIR spectra of polypropylene films

The weak band at around  $1743\text{ cm}^{-1}$  is attributed to stretching of the carboxylic group  $\text{C}=\text{O}$ , as presented in the Figure 3. Furthermore, there is a band at around  $3644\text{ cm}^{-1}$  characteristic of the  $\text{O}-\text{H}$  related to  $\text{Si}-\text{OH}$  [17]. However two peaks in the IR spectrum of modified PP were observed at around  $458\text{ cm}^{-1}$  and  $642\text{ cm}^{-1}$ . According to the literature [18-21], in the low wavenumber range typical bands of silica are clearly detected at about  $460\text{ cm}^{-1}$  and  $640\text{ cm}^{-1}$  that refers to peak attributed to vibration of cyclic  $\text{Si}-\text{O}-\text{Si}$ .

### 3.3. Differential scanning calorimetry

The DSC results for PP1 and PP2 are presented in Table 2 and Figure 4.

**Table 2.** Sample values of melting peak temperature, melt-crystallization temperature and degree of crystallinity

Samples	Melting peak temperature, $T_m$ / °C	Crystallization peak temperature, $T_c$ / °C	Melting peak temperature, $T_m$ / °C	Crystallinity 1 <sup>st</sup> melting, $X_C$ / %
PP1	$169.7 \pm 0.12$	$115.5 \pm 0.14$	$162.0 \pm 0.11$	$39.2 \pm 0.9$
PP2	$169.4 \pm 0.13$	$115.4 \pm 0.13$	$164.0 \pm 0.14$	$38.6 \pm 0.5$

$T_m$  = melt temperature;  $T_c$  = crystallization temperature;  $X_C$  = degree of crystallinity, as average of three samples

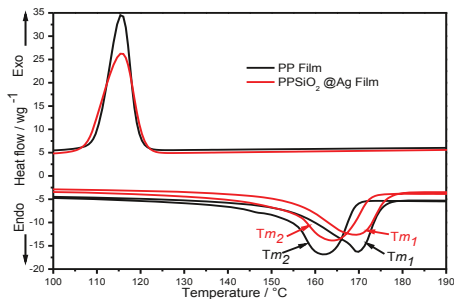


Figure 4. DSC curves in the melting of PP and PP  $\text{SiO}_2$ @Ag-NPs films

Crystallization was not affected by SiO<sub>2</sub>@Ag-NPs addition in the same sense as usually occurs with nucleating agents. As shown in Table 2 the value of the crystallinity of the PP film is similar to that of PPSiO<sub>2</sub>@Ag-NPs film.

### 3.4. X-Ray diffraction

The X-Ray diffraction patterns of the samples are shown in Table 3 and Figure 5.

**Table 3.** DRX data of PP and SiO<sub>2</sub>@Ag-NPs PP nanocomposites

Samples configurations	Crystal plane	Diffraction angle 2θ / °	Interplanar distance d / nm	Crystallites size / nm
PP	(110)α	14.72	0.600	12.4
	(300)β	16.74	0.529	19.3
	(040)α	17.52	0.506	17.3
	(130)α	19.19	0.462	14.4
	(131)+(041)β	22.30	0.398	10.7
	(150)+(060)α	26.14	0.341	14.8
	(220)α	29.32	0.304	5.5
	PPSiO <sub>2</sub> @Ag-NPs	(110)α	14.17	0.625
(040)α		16.83	0.526	11.1
(130)α		18.50	0.479	9.5
(131)+(041)β		21.99	0.404	5.2
(150)+(060)α		25.50	0.349	11.6
(220)α		28.75	0.310	7.6

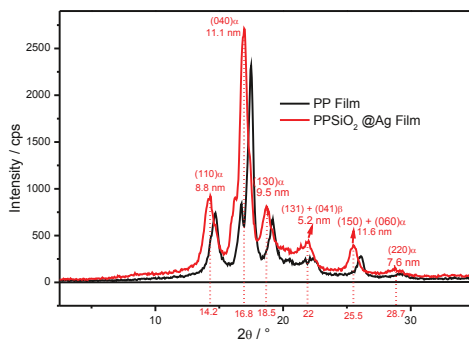


Figure 5. X-ray diffraction pattern of PP and SiO<sub>2</sub>@Ag-NPsPP films

It can be noticed two interesting peaks for PP SiO<sub>2</sub>@Ag-NPs in Figure 5. The crystal plane (131)+(041)β and (150)+(060)α showed a peak at 2θ=21.99° and 2θ= 25.50°, respectively. The first one presented a crystallite size 5.2 nm and the second one 11.6 nm. In terms of interplanar distance, the β form showed a 0.404 nm and the α form showed a 0.349 nm. According to crystallinity determination by XRD, in which the integral of halo amorphous phase is related to the integral area of the diffraction pattern, the values calculated were: 31.9 ± 1.0 for PP film and 33.6 ± 0.9 for PPSiO<sub>2</sub>@Ag film.

The formation of the  $\beta$ -phase, among other factors, is dependent of the shear level imposed to the polymer during the processing [22].

### 3.5. Antibacterial Activity

The antibacterial effects of the nanocomposites films at different concentrations of silver and silica against *Staphylococcus aureus* and *Escherichia coli*, as determined by the JIS Z 2801 technique, showed negative efficiency results versus bacteria. The result is attributed to the dimension of the carriers in which has grown the silver nanoparticle during sonification.

### Conclusion

The silver nanoparticles synthesized in SiO<sub>2</sub> carrier showed distinct results on the bactericide performance of PP@ SiO<sub>2</sub>AgNPs films. The scanning electron microscopy and dispersive spectroscopy images have shown the large dimension of silicon (5 microns) supporting nanoparticles of silver. The FTIR spectra of PPSiO<sub>2</sub>@Ag films also showed intense bands of silicon, while DSC results revealed that the crystallinity of PP film was affected by presence of SiO<sub>2</sub>@Ag. The PPSiO<sub>2</sub>@Ag film did not show efficiency to combat the bacteria *Staphylococcus aureus* and *Escherichia coli*, probable owing to the hindrance represented for the silica to nanosilver attack into the bacteria cell, our challenge for future work.

### Acknowledgements

This article was supported by CAPES PROJECT and FAPESP project n° 2014-26393-1. The authors are thankful to the Centre of science and technology of materials-CCTM/IPEN, for microscopy analysis (SEM), the technicians Mr. Eleosmar Gasparin and Nelson R. Bueno, for technical support and multipurpose gamma irradiation facility at the CTR/IPEN.

### References

- [1] C. D. Castel, M. A. S. Oviedo, S. A. Liberman, R. V. B. Oliveira, R. S. Mauler, "Solvent-assisted extrusion of polypropylene/clay nanocomposites," *Journal of Applied Polymer Science*, 121(2011), 389-394.
- [2] A. Bouaziz, M. Jaziri, F. Dalmas, V. Massardier, "Nanocomposites of silica reinforced polypropylene: Correlation between morphology and properties," *Polymer Engineering and Science*, 54(2014), 2187-2196.
- [3] M. Keijo, C. Song, *Radiation Processing of Polymer Materials and Its Industrial Applications*, John Wiley & Sons, Inc., Hoboken & New Jersey (2012).
- [4] W. L. Oliani, D. F. Parra, L. F. C. P. Lima, A. B. Lugao, "Morphological characterization of branched PP under stretching," *Polymer Bulletin*, 68(2012), 2121-2130.
- [5] S. Sanchez-Valdes, "Sonochemical deposition of silver nanoparticles on linear low density polyethylene/cyclo olefin copolymer blend films," *Polymer Bulletin*, 71(2014) 1611-1624.
- [6] F. Furno, K. S. Morley, B. Wong, B. K. Sharp, P. L. Arnold, S. M. Howdle, R. Bayston, P. D. Brown, P. D. Winship, H. J. Reid, "Silver nanoparticles and polymeric medical devices: A new approach to prevention of infection?," *Journal of Antimicrobial Chemotherapy*, 54(2004), 1019-1024.
- [7] J. R. Morones, J. L. Elechiguerra, A. Camacho, K. Holt, J. B. Kouri, J. T. Ramirez, M. J. Yacaman, "The bactericidal effect of silver nanoparticles," *Nanotechnology*, 16(2005), 2346-2353.

- [8] E. Fages, J. Pascual, O. Fenollar, D. Garcia-Sanoguera, R. Balart, "Study of Antibacterial Properties of Polypropylene Filled With Surfactant-Coated Silver Nanoparticles," *Polymer Engineering and Science*, 51(2011), 804-811.
- [9] A. Gedanken, "Using sonochemistry for the fabrication of nanomaterials," *Ultrasonics sonochemistry*, 11(2004), 47-55.
- [10] A. Matsumoto, T. Ishikawa, T. Odani, H. Oikawa, S. Okada, H. Nakanishi, "An organic/inorganic nanocomposite consisting of polymuconate and silver nanoparticles," *Macromolecular chemistry and physics*, 207 (2006), 361-369.
- [11] X. Ye, Y. Zhou, J. Chen, Y. Sun, "Deposition of silver nanoparticles on silica spheres via ultrasound irradiation," *Applied Surface Science*, 253(2007), 6264-6267.
- [12] A. B. Lugao, B. W. H. Artel, A. Yoshiga, L. F. C. P. Lima, D. F. Parra, J. R. Bueno, S. Liberman, M. Farrah, W. R. Terçariol, H. Otaguro, "Production of high melt strength polypropylene by gamma irradiation," *Radiation Physics and Chemistry*, 76(2007), 1691-1695.
- [13] A. B. Lugao, H. Otaguro, D. F. Parra, A. Yoshiga, L. F. C. P. Lima, B. W. H. Artel, S. Liberman, "Review on the production process and uses of controlled rheology polypropylene gamma radiation versus electron beam processing," *Radiation Physics Chemistry*, 76(2007), 1688-1690.
- [14] W. L. Oliani, D. F. Parra, A. B. Lugao, "UV stability of HMS-PP (high melt strength polypropylene) obtained by radiation process," *Radiation Physics and Chemistry*, 79(2010), 383-387.
- [15] D. M. Fermino, D. F. Parra, W. L. Oliani, A. B. Lugao, F. R. V. Díaz, "HMSPP nanocomposite and Brazilian bentonite properties after gamma radiation exposure," *Radiation Physics and Chemistry*, 84(2013), 176-184.
- [16] JIS Z 2801:2010 (adapted). Japanese Industrial Standard. Antimicrobial Products - Test for antimicrobial activity and efficacy.
- [17] J. G. Martinez-Colunga, S. Sanchez-Valdes, L. F. Ramos-de-Valle, L. Munoz-Jimenez, E. Ramirez-Vargas, M. C. Ibarra-Alonso, T. Lozano-Ramirez, P. G. Lafleur, "Simultaneous Polypropylene Functionalization and Nanoclay Dispersion in PP/Clay Nanocomposites using Ultrasound," *Journal of Applied Polymer Science*, (2014), 40631 (1 of 8).
- [18] N. Primeau, C. Vautey, M. Langlet, "The effect of thermal annealing on aerosol-gel deposited SiO<sub>2</sub> films: a FTIR deconvolution study", *Thin Solid Films*, 310(1997), 47-56.
- [19] J. G. M. Colunga, S. S. Valdes, L. F. R. Valle, L. M. Jimenez, E. R. Vargas, M. C. I. Alonso, T. L. Ramirez, P. G. Lafleur, "Simultaneous Polypropylene Functionalization and Nanoclay Dispersion in PP/Clay Nanocomposites using Ultrasound," *Journal of Applied Polymer Science*, 131(2014), 40631.
- [20] T. Li, S. Xiang, P. Ma, H. Bai, W. Dong, M. Chen, "Nanocomposite Hydrogel Consisting of Na-montmorillonite with Enhanced Mechanical Properties," *Journal of Polymer Science Part B: Polymer Physics*, 53(2015), 1020-1026.
- [21] E. V. D. G. Libano, L. L. Y. Visconte, E. B. A. V. Pacheco, "Propriedades térmicas de compósitos de polipropileno e bentonita organofílica," *Polímeros*, 22(2012), 430-435.
- [22] M. M. Favaro, M. C. Branciforti, R. E. S. Bretas, "A X-ray Study of  $\beta$ -Phase and Molecular Orientation in Nucleated and Non-Nucleated Injection Molded Polypropylene Resins," *Materials Research*, 12, 4, (2009), 455-464.